Original Article

Quantitative analysis of paravertebral muscle asymmetry and its correlation with spinal deformity in patients with degenerative lumbar scoliosis: a retrospective case-control study

Mengjiao Chen[1,2]^, Shundan Zhao[1,2]^, Shaoqing Chen[1,2], Yingying Huang[1,2], Zhihan Yan[1,2], Jiawei He[1,2]^

[1]Department of Radiology, The Second Affiliated Hospital and Yuying Children's Hospital of Wenzhou Medical University, Wenzhou, China; [2]Wenzhou Key Laboratory of Structural and Functional Imaging, Wenzhou, China

Contributions: (I) Conception and design: J He, M Chen; (II) Administrative support: Z Yan; (III) Provision of study materials or patients: J He, Z Yan; (IV) Collection and assembly of data: M Chen, S Zhao, S Chen, Y Huang; (V) Data analysis and interpretation: M Chen, S Zhao; (VI) Manuscript writing: All authors; (VII) Final approval of manuscript: All authors.

Correspondence to: Zhihan Yan, MD, PhD; Jiawei He, PhD. Department of Radiology, The Second Affiliated Hospital and Yuying Children's Hospital of Wenzhou Medical University, 109 Xueyuan West Road, Wenzhou, China; Wenzhou Key Laboratory of Structural and Functional Imaging, Wenzhou, China. Email: yanzhihanwz@163.com; hejw505@163.com.

Background: The degeneration and functional decline of paravertebral muscles (PVMs) are reported to be closely linked to the incidence of degenerative lumbar scoliosis (DLS), a spinal deformity of the mature skeleton. However, the functional role and degeneration of PVMs and their relationship to the development of spinal deformities remain controversial. Therefore, the present study analyzed the morphological changes in the PVMs of patients with DLS, and explored the relationship between PVM degeneration and spinal osseous parameters.

Methods: In this retrospective case-control study, we evaluated the PVM parameters of patients with DLS (n=120) and compared them with patients free of DLS (control group, n=120). The cross-sectional area (CSA) and computed tomography (CT) values of the PVM at the lumbar vertebra 1–5 levels were measured. Further, the lumbar scoliosis Cobb, lumbar lordotic, and apical vertebral rotation angles were measured on CT and radiographs in the DLS group, and the relationship between PVM changes and these factors was analyzed.

Results: In the control group, the PVM CSA and CT values differed insignificantly between the bilateral sides at all levels ($P>0.05$). In the DLS group, the CSAs of the multifidus (MF) and erector spinae (ES) were larger on the convex side than the concave side ($P>0.05$), whereas that of the psoas major (PM) was smaller on the convex side than the concave side ($P<0.05$). The CT value of the PVM was lower on the convex side at all levels ($P<0.05$). The CSA and CT values on both sides of the patients were lower in the DLS group than the control group at all levels ($P<0.05$). Further, the degree of PVM asymmetry at the apical vertebral level was positively correlated with the lumbar scoliosis ($P<0.01$) and apical vertebral rotation angles ($P<0.05$), but negatively correlated with the lumbar lordotic angle ($P<0.05$).

Conclusions: Asymmetric degeneration of the PVM was observed bilaterally in DLS patients, and the degeneration was more pronounced on the concave side than the convex side. This asymmetrical degeneration was closely associated with the severity of lumbar scoliosis, vertebral rotation, and loss of lumbar lordosis, and a stronger correlation was observed with the MF and ES than with the PM.

^ ORCID: Jiawei He, 0000-0003-1133-7429; Mengjiao Chen, 0009-0000-7893-2391; Shundan Zhao, 0009-0006-6999-6952.

Keywords: Degenerative lumbar scoliosis (DLS); asymmetric degeneration; paravertebral muscles (PVMs); cross-sectional area (CSA)

Submitted Nov 23, 2023. Accepted for publication Mar 15, 2024. Published online Apr 18, 2024.
doi: 10.21037/qims-23-1668
View this article at: https://dx.doi.org/10.21037/qims-23-1668

Introduction

Degenerative lumbar scoliosis (DLS) is a spinal deformity primarily affecting the mature skeleton and characterized by a curvature of the spine with a Cobb angle of ≥10º (1). It has emerged as a clinically significant concern, particularly among individuals aged 60 years or older (2). Most DLS patients experience symptoms such as lower back pain, leg pain, numbness, and intermittent claudication that significantly affect their quality of life (3). Most scholars attribute the pathogenesis of DLS to degenerative changes in the spinal structures, such as the intervertebral discs, facet joints, and vertebrae (4). However, paravertebral muscle (PVM) degeneration is increasingly recognized as a crucial occurrence in the disease (5,6), and the degeneration and functional decline of PVMs are closely related to the development and occurrence of DLS (7).

The PVMs can be divided into flexor and extensor muscle groups based on their functions. The lumbar back extensor muscle group primarily comprises the multifidus (MF) and erector spinae (ES) muscles, which primarily function to extend, rotate, and laterally flex the spine (8,9). In contrast, the psoas major (PM) muscle belongs to the lumbar back flexor muscle group, and primarily supports the pelvis trunk. It also prevents spine buckling and controls lordosis (10).

Computed tomography (CT) and magnetic resonance imaging (MRI) are commonly used to analyze degenerative muscle changes (11). MRI is advantageous due to its non-invasive nature and ability to clearly delineate muscle edges, but it has a longer acquisition time and higher costs than CT. Moreover, measuring fatty infiltration in MRI necessitates precise techniques and additional software, leading to lower efficiency and potential variability in the calculation results. Despite radiation exposure, CT offers the advantage of swiftly capturing high-resolution images of muscles and bones over a large area. It allows for the more accurate evaluation of vertebral rotation angles. Additionally, CT imaging uses picture archiving and communication system (PACS) workstations for image reconstruction and repeat measurements. CT-derived Hounsfield unit (HU) attenuation values provide a non-invasive measure of muscle density. These values are correlated with intramuscular fat content from biopsies, such that a lower density signifies a higher fat content (12). Ogawa *et al.* used CT scans to assess muscle degeneration by comparing cross-sectional area (CSA) ratios and CT value differences between the healthy and affected sides of patients with unilateral hip joint lesions (13). Consequently, we performed a CT-based assessment of muscle degenerative changes.

Previous research has shown that the asymmetric degeneration of PVM is a contributing factor to coronal imbalance (14). Further, a study involving 140 patients with lumbar spinal stenosis and degenerative spondylolisthesis revealed a correlation between the CSA of the MF and PM, and sagittal pelvic parameters, suggesting a correlation between PVM function and overall spinal alignment (15). These studies have reported a correlation between spinal deformity and PMV degeneration. However, the relationship between the PVMs and spinal osseous parameters remains contentious.

This retrospective study aimed to apply a CT quantitative analysis to assess the morphological changes in the PVMs of patients with DLS and to evaluate the correlation between PVM asymmetry and changes in spinal osseous parameters. The primary goal of this study was to provide valuable information for evaluating disease severity and subsequent treatment strategies. We present this article in accordance with the STROBE reporting checklist (available at https://qims.amegroups.com/article/view/10.21037/qims-23-1668/rc).

Methods

Participants

This retrospective study was included 120 patients diagnosed with DLS and treated at The Second Affiliated Hospital and Yuying Children's Hospital of Wenzhou Medical University between April 2018 and September 2022. The patients included in the study sought medical care due to low back pain. To be eligible for inclusion in

this study, patients had to meet the following inclusion criteria: (I) be aged >60 years; (II) have a Cobb angle of lumbar scoliosis in the coronal plane ≥10° on a standing posteroanterior film; and (III) have a history of lumbar spine radiography and CT scans with a scanning range that included the L1(lumbar vertebra 1)–S1(sacral vertebra 1) vertebral bodies. Patients were excluded from the study if they met any of the following exclusion criteria: (I) had other types of spinal scoliosis (including idiopathic, congenital, neurofibromatosis, or neurogenic scoliosis); (II) had a history of spinal fractures, surgery, infection, tuberculosis, tumors, or lumbar muscle injuries; and/or (III) had other systemic diseases that can affect spinal alignment, such as muscular dystrophy or Parkinson's disease. Additionally, the control group comprised 120 patients who sought medical attention for mild lower back pain during physical examinations or outpatient visits. These patients underwent examinations at the same hospital and during the same period (January 2018 to September 2022). The inclusion criteria encompassed individuals aged 60 years or older without DLS. The exclusion criteria aligned with those applied to the DLS group.

The study was conducted in accordance with the Declaration of Helsinki (as revised in 2013). The study was approved by The Second Affiliated Hospital and Yuying Children's Hospital of Wenzhou Medical University, Wenzhou, China (No. 2023-K-137-01), and the requirement of individual consent for this retrospective analysis was waived.

Imaging procedures

Standard anteroposterior radiography images were obtained using the Siemens digital radiography (Siemensysio, Siemens, Germany) and a PACS (v.3.0, Infinitt, Shanghai, China) system. The usage parameters were as follows: electric current: 500 mA; and voltage: 75 kV. Standard radiographs were obtained using a well-established protocol. Participants were instructed to maintain a natural standing posture for image acquisition. For the anteroposterior imaging, the arms were positioned along the sides of the torso, and the feet were placed side by side. For the lateral imaging, the participants placed their hands on their clavicles while simultaneously extending the buttocks and knee joints. Additionally, all patients underwent a Canon Aquilion PRIME TSX-303A 64-row 128-layer CT scan within 3 days of radiography. The scanning parameters were as follows: tube voltage: 120 kV; tube current: 100–120 mA; layer thickness: 3–5 mm; and pitch: 0.7–1.0. The images were reconstructed using a 1-mm thin layer. All the CT scans were performed with the patient in the supine position, with their upper limbs crossed over their heads, and their legs uncrossed. Patients were instructed to remain still and relaxed during the examination. All the images were transmitted through a local area network to a PACS system.

Imaging evaluation

A physician measured the lumbar scoliosis Cobb angle on standard anteroposterior radiography to assess the severity of the lateral curvature and recorded the apical vertebral level and curve direction. If the apical vertebra was in the intervertebral space, the upper vertebra was considered the apical vertebra and measured accordingly. In the DLS group, multiplanar reconstruction was performed on the PACS system along the middle plane of the vertebral arch to measure the CSAs of the ES, MF, and PM at the L1–5 levels. The system automatically generated the mean CT value of the traced region (*Figure 1A*). Each PVM CSA and CT value was measured thrice and averaged. The same data were measured at the maximum cross-sectional plane of the control group. The CSA difference index (CDI) has been used in previous studies to account for individual differences in body size, weight, and height on the muscle CSA (16). We compared the CSA and CT values of the two sides in each group to describe the PVM imbalance. Subsequently, we compared the CSA and CT values of the convex and concave sides of the PVM in patients with DLS with the average of the CSA and CT values of the control group to explore intergroup differences in PVM morphology. Similarly, we compared the CDI and CT value differences of the apical vertebral PVM with the spinal osseous parameters to determine the relationship between PVM degeneration and the severity of lumbar curvature, axial rotation and loss of lumbar lordosis as follows:

$$\text{Average CSA} = \left[\left(CSA_{left} + CSA_{right}\right)/2\right] \times 100\% \quad [1]$$

$$\text{Average CT} = \left(CT_{left} + CT_{right}\right)/2 \quad [2]$$

$$\text{CDIPM} = \left[1 - \left(CSA_{convex} / CSA_{concave}\right)\right] \times 100\% \quad [3]$$

$$\text{CDIMF / ES} = \left[1 - \left(CSA_{concave} / CSA_{convex}\right)\right] \times 100\% \quad [4]$$

$$\text{CT Value Difference} = CT_{convex} - CT_{concave} \quad [5]$$

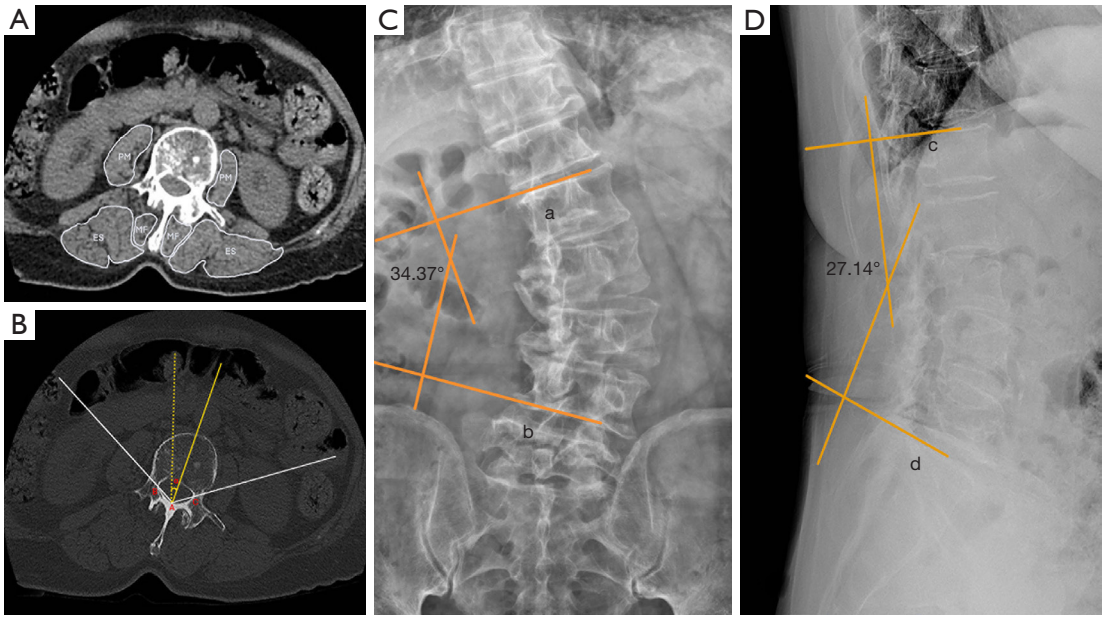

Figure 1 Degenerative lumbar scoliosis radiography. (A) Delineation of paraspinal muscles in axial CT images. (B) Axical CT; Ho's method. (A) is located at the junction of the inner surfaces of two laminae; (B) and (C) are situated at the corresponding junctions of the inner surfaces of the laminae and pedicles; the angle α between the bisector of the (BAC) angle and the sagittal plane is defined as the apical vertebral rotation angle; (C) standard anteroposterior radiography; line a is parallel to the upper endplate of the upper vertebra, while line b is parallel to the lower endplate of the lower vertebra; the angle between lines a and b is known as the Cobb angle; (D) standard lateral radiography; line c is parallel to the upper endplate of L1, while line d is parallel to the upper endplate of S1; the angle between lines c and d is known as the lumbar lordotic angle. PM, psoas major; MF, multifidus; ES, erector spinae; CT, computed tomography.

where CSAleft is the CSA of the PVM on the left side of the controls; CSAright is the CSA of the PVM on the right side of the controls; CSAconcave is the CSA of the PVM on the concave side of patients with DLS; CSAconvex is the CSA of the PVM on the convex side of patients with DLS; CDIPM is the CDI of the PM; CDIMF/ES is the CDI of the MF or ES; CTleft is the CT of the PVM on the left side of the controls; CTright is the CT of the PVM on the right side of the controls; CTconcave is the CT of the PVM on the concave side of the patients with DLS; and CTconvex is the CT of the PVM on the convex side of the patients with DLS.

We selected the vertebral level with relatively intact vertebral cortices and spinous processes from the cross-sectional CT images. Using Ho's method (17), the rotational angle of the apical vertebra was measured on axially reconstructed images, and three distinct data points were identified for the analysis; the first (*Figure 1A*) was located at the junction of the inner surfaces of two laminae, while the other two (*Figure 1B,1C*) were situated at the corresponding junctions of the inner surfaces of the laminae and pedicles. A line bisecting the (BAC) angle formed by the two laminae was then drawn computationally, allowing us to accurately define the angle of apical vertebral rotation as the angle between the line and the vertical plane drawn by the computer program (*Figure 1B*).

The lumbar scoliosis Cobb angle is defined as the angle between lines "a" and "b", which are parallel to the superior endplate of the upper vertebra and the inferior endplate of the lower vertebra, respectively (*Figure 1C*). Similarly, the lumbar lordotic angle is defined as the angle between lines "c" and "d", which are parallel to the superior endplate of L1 and the superior endplate of S1, respectively (*Figure 1D*).

Statistical analysis

The continuous data are presented as the mean ± standard deviation. All the statistical analyses were performed using SPSS, version 26 (Statistical Package for Social Sciences, IBM Corp., Chicago, IL, USA). Two-sample *t*-tests were used to compare age and body mass index (BMI) between

Table 1 Demographic characteristics of both groups

Demographics	DLS group	Control group	P value
Age (years)	69.88±5.44	69.25±5.58	0.08
BMI (kg/m^2)	23.79±3.10	24.29±3.06	0.22
Sex			0.33
Male	34	41	
Female	86	79	

Values are given as the number, or mean ± standard deviation. DLS, degenerative lumbar scoliosis; BMI, body mass index.

the groups, while chi-square tests were used to compare sex. Paired *t*-tests were used to compare the CSA and CT values of the PVM between the two sides of the patients in each group. Independent sample *t*-tests were used to evaluate the differences in the CSA and CT values between the two sides of the patients with DLS and the mean CSA and CT values of the control group. A Pearson's correlation analysis was conducted to examine the relationship between the degree of PVM asymmetry and the spinal osseous parameters in the DLS group. A significance level of α=0.05 was used, and a P value <0.05 was considered statistically significant.

Results

All the patients were divided into the DLS and control groups based on the presence or absence of DLS. The DLS group comprised 120 patients, including 34 males and 86 females, with a mean age of 69.88±5.44 years, and a BMI of 23.79±3.10 kg/m^2. Among them, 88 and 32 had left- and right-sided curvatures, respectively, with the primary curve apex located at L1–2 intervertebral discs in 1 (0.83%), L2 vertebra in 17 (14.17%), L2–3 intervertebral disc in 21 (17.5%), L3 vertebra in 60 (50.00%), L3–4 intervertebral disc in 17 (14.17%), and L4 vertebra in 4 (3.33%) patients. The mean lumbar scoliosis Cobb angle was 18.77°±6.68°, and that of the lumbar lordotic angle was 33.28°±10.67°. Further, the apical vertebral rotation angle was 14.79°±5.18°. Similarly, the control group comprised 120 patients, including 41 males and 79 females, with a mean age of 69.25±5.58 years and a BMI of 24.29±3.06 kg/m^2. The DLS and control groups did not differ significantly in terms of age, sex, and BMI (*Table 1*).

The imaging parameters for the muscles on the concave and convex sides were measured at the L1–5 levels in both groups. In the DLS group, the results showed that the CSA of the PM was significantly greater on the concave side than the convex side (P<0.05), whereas those of the MF and ES were significantly greater on the convex side than the concave side (P<0.05). Additionally, the CT values of the MF, ES, and PM were significantly higher on the convex side than the concave side (P<0.05) (*Table 2*). In the control group, the results revealed no differences in the CSA or CT values of the MF, ES, or PM between the left and right sides (P>0.05) (*Table 3*).

The CSAs of the MF, ES, and PM on the convex side at the L1–5 levels were significantly lower in the DLS group than the control group (P<0.05). In addition, the CSA of the MF and ES on the concave side at the L1–5 levels were significantly lower in the DLS group than the control group (P<0.05), whereas those of the PMs on the concave side at the L1–5 levels between the DLS and control groups showed no significant difference (P>0.05) (*Table 4*). The CT values of the PVMs on the concave and convex sides at the L1–5 levels were significantly lower in the DLS group than the control group (P<0.05) (*Table 5*).

According to the correlation analysis, the CDI and CT value differences of the PM, MF, and ES at the apical vertebra level were positively correlated with the lumbar scoliosis Cobb angle (r=0.341, 0.261, 0.455, 0.428, 0.441, and 0.394, respectively; P<0.01) (*Figure 2*), and the apical vertebral rotation angle (r=0.207, 0.319, 0.254, 0.346, 0.389, 0.424, respectively; P<0.05) in the DLS group (*Figure 3*). Conversely, these differences were negatively correlated with the lumbar lordotic angle (r=–0.247, –0.183, –0.365, –0.327, –0.312, –0.297, respectively; P<0.05) (*Figure 4*). Moreover, the MF and ES correlation coefficients were greater than those of the PM.

Discussion

The PVMs play crucial roles in supporting and stabilizing the spine and regulating posture maintenance and movement (18,19). Most recent research has focused on the role of the vertebral body and intervertebral disc degeneration in DLS (20-22), and only limited attention has been paid to the role of the PVM. Therefore, in the present study, we used CT to analyze the degree of PVM degeneration in patients with DLS and investigated its relationship with spinal osseous parameters. Our results demonstrated that PVMs undergo asymmetric degeneration, which is correlated with the occurrence of lumbar scoliosis, vertebral rotation, and loss of lumbar lordosis. These findings highlight the importance of examining the role of PVM in DLS and suggest that

Table 2 Imaging parameters of PVM on the concave side and convex side in the DLS group

Level	PVM	CSA (mm^2)			CT value (HU)		
		Convex side	Concave side	P value	Convex side	Concave side	P value
L1	PM	104.34±63.99	133.33±73.94	<0.001***	31.97±11.89	23.52±13.83	<0.001***
	MF	185.02±57.46	165.90±52.53	<0.001***	29.42±15.32	22.83±18.27	<0.001**
	ES	1,365.29±412.46	1,269.31±359.97	<0.001***	32.07±13.65	30.30±13.94	<0.05*
L2	PM	317.12±126.32	383.07±138.13	<0.001***	41.05±6.65	32.71±9.43	<0.001***
	MF	249.85±86.00	220.04±80.71	<0.001***	34.66±19.26	19.72±19.13	<0.001***
	ES	1,440.85±382.62	1,347.57±403.79	<0.001***	30.44±14.09	27.97±13.02	<0.05*
L3	PM	550.19±193.76	678.94±225.76	<0.001***	41.70±6.02	35.67±8.35	<0.001***
	MF	346.78±120.54	311.32±119.19	<0.001***	32.52±16.23	22.04±17.36	<0.001***
	ES	1,271.97±354.18	1,216.69±343.97	<0.001***	30.73±12.20	26.10±13.24	< 0.01**
L4	PM	726.95±219.51	878.58±232.72	<0.001***	40.95±6.83	37.49±7.82	<0.001**
	MF	505.43±168.10	450.00±157.40	<0.001***	23.57±20.49	23.91±18.74	0.781
	ES	1,012.72±290.50	975.86±281.74	<0.05*	27.89±12.57	25.70±14.87	<0.05*
L5	PM	763.71±256.05	899.27±262.11	<0.001***	40.99±7.04	39.52±7.28	<0.05*
	MF	570.00±156.23	540.69±145.37	<0.001***	22.81±19.32	23.19±20.76	0.766
	ES	488.43±236.98	500.68±243.12	0.38	17.19±13.57	14.25±18.21	<0.05*

Values are given as the mean ± standard deviation. *, P≤0.05; **, P≤0.01; ***, P≤0.001. PVM, paravertebral muscle; DLS, degenerative lumbar scoliosis; CSA, cross-sectional area; CT, computed tomography; HU, Hounsfield unit; PM, psoas major; MF, multifidus; ES, erector spinae.

Table 3 Imaging parameters of PVM on the left and right side in the control group

Level	PVM	CSA (mm^2)			CT value (HU)		
		Left side	Right side	P value	Left side	Right side	P value
L1	PM	125.59±68.77	123.09±67.65	0.10	31.01±10.84	31.32±9.59	0.56
	MF	198.58±48.23	199.47±49.91	0.57	30.55±13.46	30.11±13.64	0.34
	ES	1,498.39±354.51	1,483.18±355.36	0.13	35.31±12.02	35.29±11.27	0.96
L2	PM	373.87±153.27	372.72±156.89	0.72	40.81±6.16	40.78±6.69	0.94
	MF	255.99±66.86	254.85±68.05	0.62	31.44±13.25	30.85±13.47	0.19
	ES	1,622.37±373.71	1,605.45±373.83	0.13	34.13±12.84	33.65±12.76	0.14
L3	PM	658.51±224.46	655.14±230.67	0.47	42.90±5.62	43.42±5.73	0.21
	MF	378.37±109.54	381.49±127.04	0.64	36.35±8.80	35.64±9.59	0.05
	ES	1,456.03±343.77	1,444.46±350.08	0.19	33.99±8.51	33.59±9.20	0.24
L4	PM	870.93±277.19	868.25±278.01	0.70	42.36±6.13	42.83±5.52	0.17
	MF	553.61±139.70	556.18±140.98	0.58	30.94±12.93	30.20±12.95	0.06
	ES	1,090.58±260.51	1,077.01±263.45	0.09	31.56±9.94	30.89±10.51	0.06
L5	PM	927.91±284.71	928.83±300.57	0.90	42.40±5.75	42.87±5.47	0.08
	MF	630.01±138.64	621.49±132.41	0.07	30.30±15.72	30.75±15.39	0.39
	ES	543.16±195.17	541.89±189.76	0.83	18.49±14.22	18.28±14.02	0.74

Values are given as the mean ± standard deviation. PVM, paravertebral muscle; CSA, cross-sectional area; CT, computed tomography; HU, Hounsfield unit; PM, psoas major; MF, multifidus; ES, erector spinae.

Table 4 CSA of the PVM at the L1–L5 levels between the DLS group and control group

Level	PVM	CSA (mm^2)			P value	
		CSA_{convex}	$CSA_{concave}$	Average CSA	CSA_{convex} *vs.* average CSA	$CSA_{concave}$ *vs.* average CSA
L1	PM	104.34±63.99	133.33±73.94	124.34±67.70	<0.05*	0.32
	MF	185.02±57.46	165.90±52.53	199.03±48.31	<0.05*	<0.001***
	ES	1,365.29±412.46	1,269.31±359.97	1,490.78±350.65	<0.05*	<0.001***
L2	PM	317.12±126.32	383.07±138.13	373.30±154.04	<0.01**	0.60
	MF	249.85±86.00	220.04±80.71	255.42±66.26	0.57	<0.001***
	ES	1,440.85±382.62	1,347.57±403.79	1,613.91±368.63	<0.001***	<0.001***
L3	PM	550.19±193.76	678.94±225.76	657.24±226.75	<0.001***	0.45
	MF	346.78±120.54	311.32±119.19	379.93±112.85	<0.05*	<0.001***
	ES	1,271.97±354.18	1,216.69±343.97	1,450.24±343.52	<0.001***	<0.001***
L4	PM	726.95±219.51	878.58±232.72	869.59±274.96	<0.001***	0.78
	MF	505.43±168.10	450.00±157.40	554.90±137.92	<0.05*	<0.001***
	ES	1,012.72±290.50	975.86±281.74	1,083.79±258.30	<0.05*	<0.01**
L5	PM	763.71±256.05	899.27±262.11	928.37±289.84	<0.001***	0.41
	MF	570.00±156.23	540.69±145.37	625.75±133.04	0.003**	<0.001***
	ES	488.43±236.98	500.68±243.12	542.52±189.65	0.05	0.13

Values are given as the mean ± standard deviation. *, P≤0.05; **, P≤0.01; ***, P≤0.001. CSA, cross-sectional area; PVM, paravertebral muscle; DLS, degenerative lumbar scoliosis; CSA_{convex}, CSA of the PVM on the convex side of patients with DLS; $CSA_{concave}$, CSA of the PVM on the concave side of patients with DLS; PM, psoas major; MF, multifidus; ES, erector spinae.

Table 5 CT value of the PVM at the L1–L5 levels between the DLS group and control group

Level	PVM	CT value (HU)			P value	
		CT_{convex}	$CT_{concave}$	Average CT value	CT_{convex} *vs.* average CT	$CT_{concave}$ *vs.* average CT
L1	PM	31.97±11.89	23.52±13.83	31.16±9.80	0.56	<0.001***
	MF	29.42±15.32	22.83±18.27	30.33±13.31	0.62	<0.001***
	ES	32.07±13.65	30.30±13.94	35.30±11.45	<0.05*	<0.01**
L2	PM	41.05±6.65	32.71±9.43	40.79±5.89	0.74	<0.001***
	MF	34.66±19.26	19.72±19.13	31.14±13.13	0.10	<0.001***
	ES	30.44±14.09	27.97±13.02	33.89±12.68	<0.05*	<0.001***
L3	PM	41.70±6.02	35.67±8.35	43.16±5.20	<0.05*	<0.001***
	MF	32.52±16.23	22.04±17.36	35.99±8.97	<0.05*	<0.001***
	ES	30.73±12.20	26.10±13.24	33.79±8.65	<0.05*	<0.001***
L4	PM	40.95±6.83	37.49±7.82	42.59±5.53	<0.05*	<0.001***
	MF	23.57±20.49	23.91±18.74	30.57±12.74	<0.01**	<0.001***
	ES	27.89±12.57	25.70±14.87	31.23±10.03	<0.05*	<0.001***
L5	PM	40.99±7.04	39.52±7.28	42.64±5.41	<0.05*	<0.001***
	MF	22.81±19.32	23.19±20.76	30.53±15.28	<0.001***	<0.01**
	ES	17.19±13.57	14.25±18.21	18.38±13.71	0.50	<0.05*

Values are given as the mean ± standard deviation. *, P≤0.05; **, P≤0.01; ***, P≤0.001. CT, computed tomography; PVM, paravertebral muscle; DLS, degenerative lumbar scoliosis; HU, Hounsfield unit; CT_{convex}, CT of the PVM on the convex side of the patients with DLS; $CT_{concave}$, CT of the PVM on the concave side of the patients with DLS; PM, psoas major; MF, multifidus; ES, erector spinae.

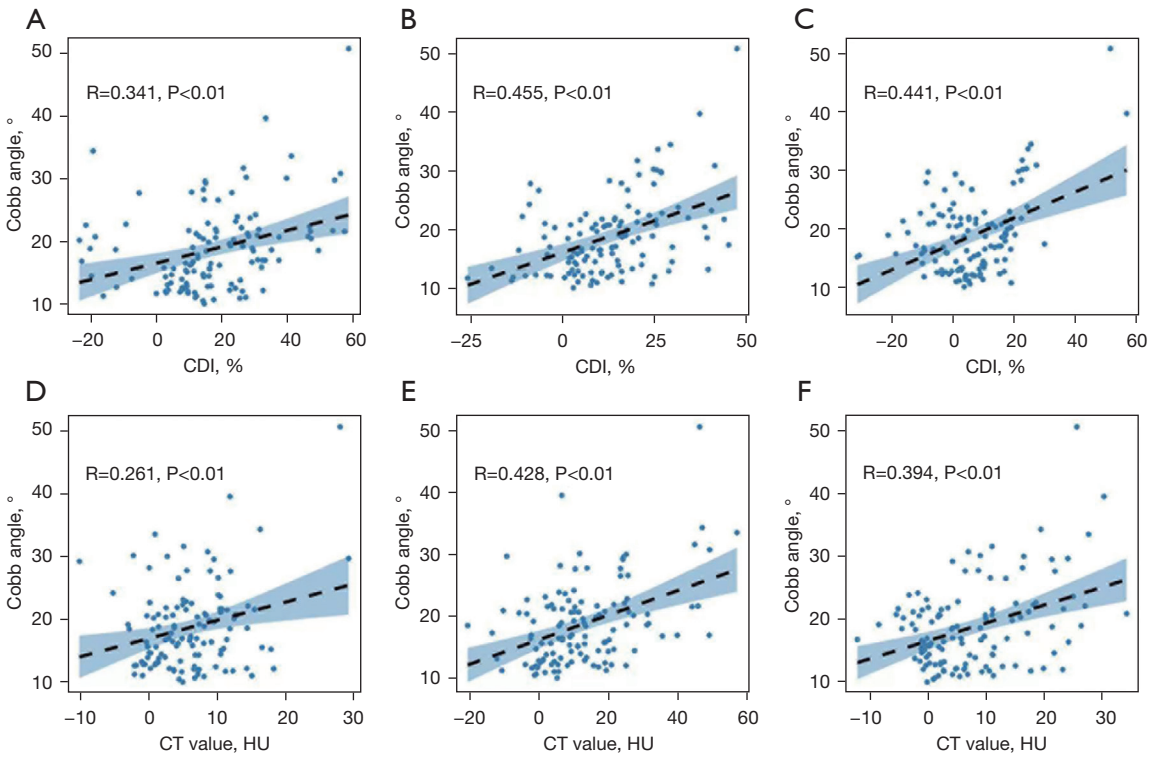

Figure 2 The correlation between lumbar scoliosis Cobb's angle and asymmetric degree of the PVM at the apical vertebrae level. (A) CDI of the PM; (B) CDI of the MF; (C) CDI of the ES; (D) CT difference value of the PM; (E) CT difference value of the MF; (F) CT difference value of the ES. CDI, CSA difference index; PVM, paravertebral muscle; PM, psoas major; MF, multifidus; ES, erector spinae; CT, computed tomography; CSA, cross-sectional area; HU, Hounsfield unit.

PVMs should be considered in clinical assessments and treatment plans for this condition.

In the control group, there were no significant differences in the CSA and degree of fat infiltration of the PVMs on both sides, which indicates that the muscle performance and stress load of the bilateral PVM in normal individuals were similar under physiological conditions. In the DLS group, the CSAs of the MF and ES were smaller on the concave side than the convex side, and fat infiltration was greater on the concave side than the convex side. Previous research showed that the diameter of muscle fibers and the number of cell nuclei were decreased on the concave side of the DLS group, indicating the location of the PVM degeneration (23). In addition, electromyography studies have shown that muscle activity of the spinal curvature is lower on the concave side, while that on the convex side increases after stretching, causing asymmetrical changes in the PVM (24). These findings are consistent with our results.

As the extensor muscles of the lumbar spine, the ES and MF are subject to a higher stress load. Compared to the PMVs on the concave side, the PVMs on the convex side work continuously, inducing compensatory hypertrophy. After the shortening of the concave side muscles, their tension and activity decreases, causing disuse atrophy, and fat infiltration increases. Therefore, we speculate that the asymmetric alterations in the MF and ES may be associated with biomechanical changes in the muscles. The difference in fat infiltration between the bilateral PMs was consistent with the aforementioned theory; however, the CSA was larger on the concave side than the convex side. The PM is a lengthy spindle-shaped muscle, primarily facilitating flexion with a comparatively longer stride that endures lower levels of stress loading than the posterior extensor muscles, such as the MF and ES (25). Therefore, the biomechanical changes in the PM are comparatively less pronounced than those observed in the posterior extensor muscles. Considering that the curvature of the spinal column in the coronal plane results in asymmetry in the arc length of the convex and concave sides, the muscles on the convex side may become

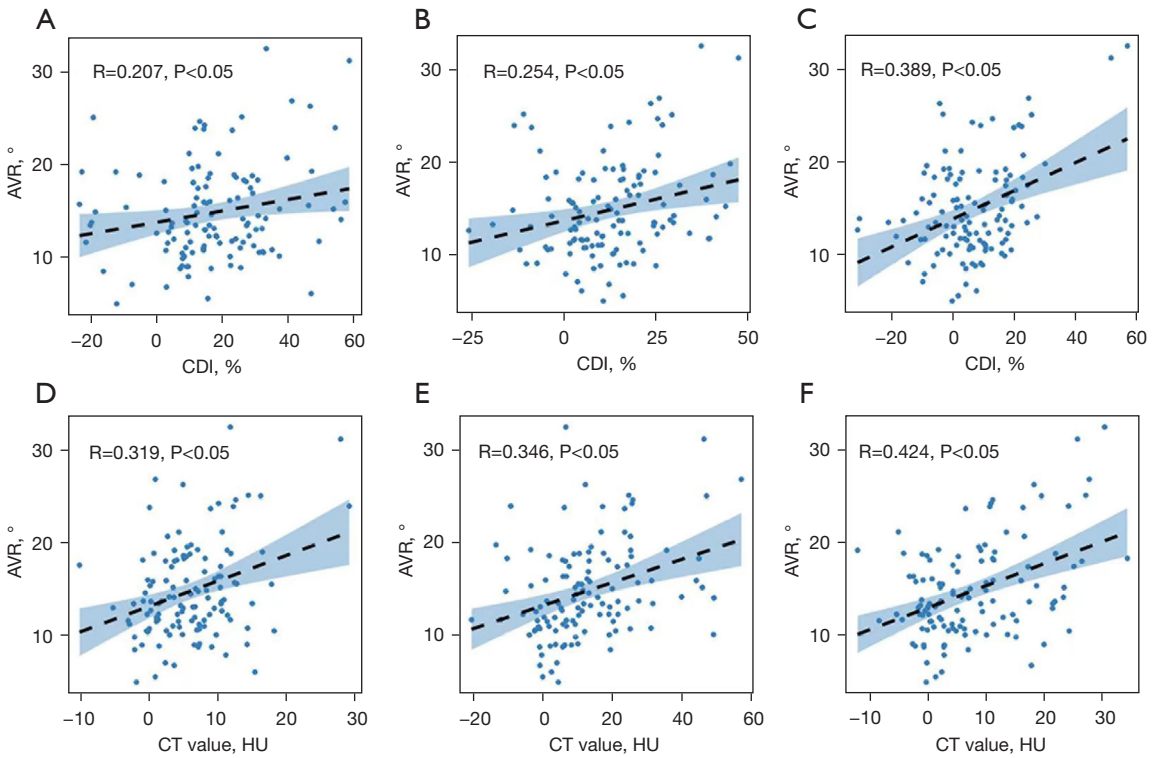

Figure 3 The correlation between the apical vertebral rotation angle and asymmetric degree of the PVM at the apical vertebrae level. (A) CDI of the PM; (B) CDI of the MF; (C) CDI of the ES; (D) CT difference value of the PM; (E) CT difference value of the MF; (F) CT difference value of the ES. AVR, apical vertebral rotation; CDI, CSA difference index; CT, computed tomography; HU, Hounsfield unit; PVM, paravertebral muscle; PM, psoas major; MF, multifidus; ES, erector spinae; CSA, cross-sectional area.

stretched, elongated, and thinned out, while those on the concave side may have become compressed, shortened, and thickened. Therefore, we speculate that the asymmetric changes in the CSA of the PM are primarily associated with changes in the spinal position.

In general, the results of this study indicate that the DLS group exhibited higher levels of fat infiltration in the PM, ES and MF bilaterally compared to the control group. Further, the CSA of the concave and convex sides in the MF and ES, as well as the convex side in the PM, were smaller in the DLS group compared to the control group. This study revealed that much greater PVM degeneration occurred on the convex and concave sides in the DLS group compared with the control group. PVM degeneration may be associated with lumbar kyphosis, lateral curvature, vertebral rotation, and the muscles being under a higher load condition (26). Previous research compared the differences in the CSAs of the PVMs between patients with DLS and healthy controls, and the CSAs of the PVMs on both sides were smaller in patients with DLS (27). A study on changes in PVM fiber types in patients with spinal deformity reported that the degree of muscle fat infiltration was significantly higher in patients with scoliosis than in those in the control group (28). Muscle fat accumulation can promote the conversion of type I (slow-twitch oxidative) to type IIb (fast-twitch glycolytic) fibers, decreasing effective muscle contraction ability and muscle performance (29).

DLS is a three-dimensional deformity characterized by the lateral displacement of vertebral bodies, vertebral slippage, and vertebral rotation in the coronal, sagittal, and axial planes, respectively (30). When asymmetric changes occur in the bone and ligaments due to degeneration, and spinal stability maintenance is lost, the muscle system is activated to compensate for the instability partially. However, prolonged muscle compensation may accelerate muscle degeneration (31). Overall, our results demonstrate that the severity of asymmetry in the MF, ES, and PM was positively correlated with the degree of lumbar scoliosis, axial rotation,

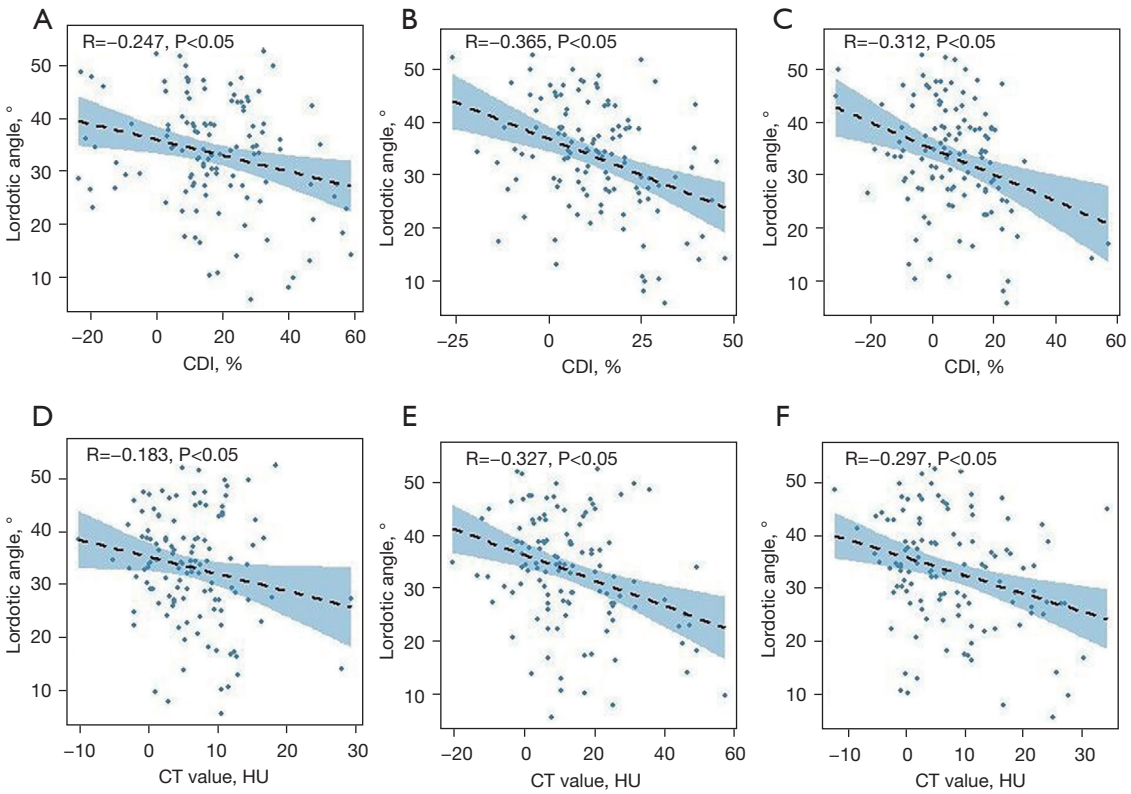

Figure 4 The correlation between the lumbar lordotic angle and asymmetric degree of the PVM at the apical vertebrae level. (A) CDI of the PM; (B) CDI of the MF; (C) CDI of the ES; (D) CT difference value of the PM; (E) CT difference value of the MF; (F) CT difference value of the ES. CDI, CSA difference index; CT, computed tomography; HU, Hounsfield unit; PVM, paravertebral muscle; PM, psoas major; MF, multifidus; ES, erector spinae; CSA, cross-sectional area.

and loss of lumbar lordosis in patients with DLS.

Asymmetric PVM degeneration may cause uneven force distribution in the coronal, sagittal, and axial planes of the spine, affecting the balance of the spine and exacerbating the degree of spinal deformity. Cheung *et al.* (32) previously reported significant differences in the electromyogram ratio of the PVM between the concave and convex sides at the apex and two-end vertebrae of the scoliotic curve, and observed greater differences in patients who experienced faster progression. Jiang *et al.* (33) further suggested that the asymmetry index of muscle volume in patients with adolescent idiopathic scoliosis is related to the degree of lumbar scoliosis, whereas that of fat degeneration is related to apical vertebral translation and the degree of lumbar scoliosis. These findings either directly or indirectly support our view that PVMs are crucial in maintaining the stability of the spine and that their degeneration may be related to the development of DLS. Therefore, we propose that personalized training targeting PVM function could help to adjust the muscle balance on both sides of the spine, which may slow the progression of PVM asymmetric degeneration and delay the development of lumbar scoliosis, apical vertebral rotation, and loss of lumbar lordosis. This personalized training could be programmed for individual patients to ensure optimal treatment outcomes.

In addition, this study revealed that the correlation between the degree of asymmetry in the PM and spinal osseous parameters was weaker than that between the MF and ES. Patients with DLS exhibit significant imbalances in their flexion-extension muscle strength, with a predominant decrease in the strength of the extensor muscles (27), possibly resulting in a decrease lumbar stability. The MF and ES primarily regulate the lateral flexion and rotational movements of the spinal column, while the PM serves as a stabilizer for the hip joint and the core of the body.

Moal *et al.* (34) studied the volume and fat infiltration

of the PVM in adult degenerative scoliosis and found that the fat infiltration rate of the lumbar extensor muscles was higher than that of the lumbar flexor muscles, and that muscle volume was negatively correlated with the fat infiltration rate. Takemitsu *et al.* (25) compared the trunk muscle strength between patients with lumbar degenerative kyphosis (LDK) and those without DLS. Specifically, they conducted an isokinetic analysis and found that the lumbar extensors of patients with LDK were significantly weaker than their lumbar flexors. Additionally, they also have reported that the lumbar extensors in LDK patients demonstrated significant atrophy and fatty infiltration using CT imaging. We propose that the coordinated action of the lumbar back muscles maintains spinal stability. When degenerative scoliosis occurs, the extensors demonstrate a more pronounced degree of fatty infiltration and atrophy than the flexors.

This study provides a novel perspective on DLS, suggesting that its development may be associated not only with asymmetrical changes in concave and convex side PVM, but also with imbalances between the flexor and extensor muscles of the lumbar spine. These findings have valuable implications for spinal health issues in the elderly population. Hence, we propose targeted neuromuscular electrical stimulation therapy for the patient's back muscles, involving the personalized adjustment of stimulation parameters and electrode placement (35). This intervention aims to enhance muscle strength and prevent muscle atrophy with the ultimate goal of effectively promoting functional recovery and improving the quality of life of individuals with DLS.

This study had some limitations. As previously mentioned, DLS is a three-dimensional deformity. However, the measurements of CSA and CT values are conducted in a two-dimensional plane, which may hinder the accurate representation of muscle volume and the extent of fat infiltration. Consequently, further application of three-dimensional imaging techniques is warranted. By acquiring continuous cross-sectional images of the PVM and subsequently performing three-dimensional reconstruction, detailed information regarding the volume and shape of the PVM can be provided. Additionally, we employed CT imaging to assess muscle degeneration, and the measured muscle HU values indirectly reflect muscle fat content. However, CT lacks the ability to accurately differentiate the distribution of intramuscular fat, such as intermuscular adipose tissue or intramyocellular fat as precisely as MRI does, while also raising the concern of radiation exposure. Moreover, the generalizability of these research findings may be limited due to the specific characteristics of the elderly population and the presence of only a weak to moderate correlation between the asymmetric degeneration of PVM and spinal osseous parameters. Therefore, future studies should expand the sample size by including DLS patients of different age groups and patients with different severities and conduct a multi-factor analysis to improve the applicability and generality of the findings. Finally, our study was retrospective and involved only static measurements and no dynamic analysis, which limited our ability to determine a causal relationship between PVM degeneration and lumbar scoliosis. Future research endeavors will include the dynamic assessment of PVM before and after exercise, and prospective cohort studies to elucidate potential causal relationships. This will provide clinicians with more effective strategies to prevent, diagnose, and treat DLS.

Conclusions

Our study found that asymmetric degeneration of the PVM was noted bilaterally in the DLS group but was significantly greater on the concave side than the convex side. This asymmetrical degeneration was closely associated with the severity of lumbar scoliosis, vertebral rotation, and loss of lumbar lordosis, with a stronger correlation observed with the MF and ES than with the PM. These findings could influence clinical assessments, provide subsequent treatment approaches for DLS, and may offer new avenues for improving patient outcomes.

Acknowledgments

The authors would like to thank all the patients who participated in this study. Their cooperation and involvement were crucial in gathering the necessary data and advancing our understanding in the field. Further, the authors would also like to express their gratitude to the dedicated staff at The Second Affiliated Hospital and Yuying Children's Hospital of Wenzhou Medical University, Wenzhou, China. Their assistance, support, and expertise greatly contributed to the smooth execution of this research project.

Funding: None.

Footnote

Reporting Checklist: The authors have completed the

STROBE reporting checklist. Available at https://qims.amegroups.com/article/view/10.21037/qims-23-1668/rc

Conflicts of Interest: All authors have completed the ICMJE uniform disclosure form (available at https://qims.amegroups.com/article/view/10.21037/qims-23-1668/coif). The authors have no conflicts of interest to declare.

Ethical Statement: The authors are accountable for all aspects of the work in ensuring that questions related to the accuracy or integrity of any part of the work are appropriately investigated and resolved. The study was conducted in accordance with the Declaration of Helsinki (as revised in 2013). The study was approved by The Second Affiliated Hospital and Yuying Children's Hospital of Wenzhou Medical University, Wenzhou, China (No. 2023-K-137-01), and the requirement of individual consent for this retrospective analysis was waived.

References

1. Wong E, Altaf F, Oh LJ, Gray RJ. Adult Degenerative Lumbar Scoliosis. Orthopedics 2017;40:e930-9.
2. Simon MJK, Halm HFH, Quante M. Perioperative complications after surgical treatment in degenerative adult de novo scoliosis. BMC Musculoskelet Disord 2018;19:10.
3. Rustenburg CME, Kingma I, Holewijn RM, Faraj SSA, van der Veen A, Bisschop A, de Kleuver M, Emanuel KS. Biomechanical properties in motion of lumbar spines with degenerative scoliosis. J Biomech 2020;102:109495.
4. Yang F, Liu Z, Zhu Y, Zhu Q, Zhang B. Imaging of muscle and adipose tissue in the spine: A narrative review. Medicine (Baltimore) 2022;101:e32051.
5. Sun XY, Kong C, Lu SB, Wang W, Cheng YZ, Sun SY, Guo MC, Ding JZ. The Parallelogram Effect of Degenerative Structures Around the Apical Vertebra in Patients with Adult Degenerative Scoliosis: The Influence of Asymmetric Degeneration and Diagonal Degeneration on the Severity of Deformity. Med Sci Monit 2019;25:3435-45.
6. Yagi M, Hosogane N, Watanabe K, Asazuma T, Matsumoto M; . The paravertebral muscle and psoas for the maintenance of global spinal alignment in patient with degenerative lumbar scoliosis. Spine J 2016;16:451-8.
7. Jun HS, Kim JH, Ahn JH, Chang IB, Song JH, Kim TH, Park MS, Chan Kim Y, Kim SW, Oh JK, Yoon DH. The Effect of Lumbar Spinal Muscle on Spinal Sagittal Alignment: Evaluating Muscle Quantity and Quality. Neurosurgery 2016;79:847-55.
8. Kader DF, Wardlaw D, Smith FW. Correlation between the MRI changes in the lumbar multifidus muscles and leg pain. Clin Radiol 2000;55:145-9.
9. Bierry G, Kremer S, Kellner F, Abu Eid M, Bogorin A, Dietemann JL. Disorders of paravertebral lumbar muscles: from pathology to cross-sectional imaging. Skeletal Radiol 2008;37:967-77.
10. Penning L. Psoas muscle and lumbar spine stability: a concept uniting existing controversies. Critical review and hypothesis. Eur Spine J 2000;9:577-85.
11. Wang FZ, Sun H, Zhou J, Sun LL, Pan SN. Reliability and Validity of Abdominal Skeletal Muscle Area Measurement Using Magnetic Resonance Imaging. Acad Radiol 2021;28:1692-8.
12. Taaffe DR, Henwood TR, Nalls MA, Walker DG, Lang TF, Harris TB. Alterations in muscle attenuation following detraining and retraining in resistance-trained older adults. Gerontology 2009;55:217-23.
13. Ogawa T, Takao M, Otake Y, Yokota F, Hamada H, Sakai T, Sato Y, Sugano N. Validation study of the CT-based cross-sectional evaluation of muscular atrophy and fatty degeneration around the pelvis and the femur. J Orthop Sci 2020;25:139-44.
14. Kiram A, Hu Z, Man GC, Ma H, Li J, Xu Y, Qian Z, Zhu Z, Liu Z, Qiu Y. The role of paraspinal muscle degeneration in coronal imbalance in patients with degenerative scoliosis. Quant Imaging Med Surg 2022;12:5101-13.
15. Hiyama A, Katoh H, Sakai D, Tanaka M, Sato M, Watanabe M. The correlation analysis between sagittal alignment and cross-sectional area of paraspinal muscle in patients with lumbar spinal stenosis and degenerative spondylolisthesis. BMC Musculoskelet Disord 2019;20:352.
16. Kim H, Lee CK, Yeom JS, Lee JH, Cho JH, Shin SI, Lee HJ, Chang BS. Asymmetry of the cross-sectional area of paravertebral and psoas muscle in patients with

degenerative scoliosis. Eur Spine J 2013;22:1332-8.
17. Ho EK, Upadhyay SS, Chan FL, Hsu LC, Leong JC. New methods of measuring vertebral rotation from computed tomographic scans. An intraobserver and interobserver study on girls with scoliosis. Spine (Phila Pa 1976) 1993;18:1173-7.
18. Xie D, Zhang J, Ding W, Yang S, Yang D, Ma L, Zhang J. Abnormal change of paravertebral muscle in adult degenerative scoliosis and its association with bony structural parameters. Eur Spine J 2019;28:1626-37.
19. Yang H, Li Z, Hai Y, Zhang H. The role of lumbosacral paraspinal muscle degeneration and low vertebral bone mineral density on distal instrumentation-related problems following long-instrumented spinal fusion for degenerative lumbar scoliosis: a retrospective cohort study. Quant Imaging Med Surg 2023;13:4475-92.
20. Zheng J, Yang Y, Cheng B, Cook D. Exploring the pathological role of intervertebral disc and facet joint in the development of degenerative scoliosis by biomechanical methods. Clin Biomech (Bristol, Avon) 2019;70:83-8.
21. Aebi M. The adult scoliosis. Eur Spine J 2005;14:925-48.
22. de Vries AA, Mullender MG, Pluymakers WJ, Castelein RM, van Royen BJ. Spinal decompensation in degenerative lumbar scoliosis. Eur Spine J 2010;19:1540-4.
23. Shafaq N, Suzuki A, Matsumura A, Terai H, Toyoda H, Yasuda H, Ibrahim M, Nakamura H. Asymmetric degeneration of paravertebral muscles in patients with degenerative lumbar scoliosis. Spine (Phila Pa 1976) 2012;37:1398-406.
24. Wilczyński J. Relationship between Muscle Tone of the Erector Spinae and the Concave and Convex Sides of Spinal Curvature in Low-Grade Scoliosis among Children. Children (Basel) 2021;8:1168.
25. Takemitsu Y, Harada Y, Iwahara T, Miyamoto M, Miyatake Y. Lumbar degenerative kyphosis. Clinical, radiological and epidemiological studies. Spine (Phila Pa 1976) 1988;13:1317-26.
26. Liang R, Zhang Y, Liu C, Wang W, Zhang W. Changes and clinical significance of paravertebral muscle cross-sectional area and fatty degree in degenerative lumbar scoliosis. Journal of Spinal Surgery 2021;19:243-6.
27. Banno T, Yamato Y, Hasegawa T, Kobayashi S, Togawa D, Oe S, Mihara Y, Kurosu K, Yamamoto N, Matsuyama Y. Assessment of the Cross-Sectional Areas of the Psoas Major and Multifidus Muscles in Patients With Adult Spinal Deformity: A Case-Control Study. Clin Spine Surg 2017;30:E968-73.
28. Mannion AF, Meier M, Grob D, Müntener M. Paraspinal muscle fibre type alterations associated with scoliosis: an old problem revisited with new evidence. Eur Spine J 1998;7:289-93.
29. Hamrick MW, McGee-Lawrence ME, Frechette DM. Fatty Infiltration of Skeletal Muscle: Mechanisms and Comparisons with Bone Marrow Adiposity. Front Endocrinol (Lausanne) 2016;7:69.
30. He JW, Bai GH, Ye XJ, Liu K, Yan ZH, Zhang X, Wang XY, Huang YX, Yu ZK. A comparative study of axis-line-distance technique and Cobb method on assessing the curative effect on scoliosis. Eur Spine J 2012;21:1075-81.
31. Schwab F, Patel A, Ungar B, Farcy JP, Lafage V. Adult spinal deformity-postoperative standing imbalance: how much can you tolerate? An overview of key parameters in assessing alignment and planning corrective surgery. Spine (Phila Pa 1976) 2010;35:2224-31.
32. Cheung J, Halbertsma JP, Veldhuizen AG, Sluiter WJ, Maurits NM, Cool JC, van Horn JR. A preliminary study on electromyographic analysis of the paraspinal musculature in idiopathic scoliosis. Eur Spine J 2005;14:130-7.
33. Jiang J, Meng Y, Jin X, Zhang C, Zhao J, Wang C, Gao R, Zhou X. Volumetric and Fatty Infiltration Imbalance of Deep Paravertebral Muscles in Adolescent Idiopathic Scoliosis. Med Sci Monit 2017;23:2089-95.
34. Moal B, Bronsard N, Raya JG, Vital JM, Schwab F, Skalli W, Lafage V. Volume and fat infiltration of spino-pelvic musculature in adults with spinal deformity. World J Orthop 2015;6:727-37.
35. Curtin M, Lowery MM. Musculoskeletal modelling of muscle activation and applied external forces for the correction of scoliosis. J Neuroeng Rehabil 2014;11:52.

Cite this article as: Chen M, Zhao S, Chen S, Huang Y, Yan Z, He J. Quantitative analysis of paravertebral muscle asymmetry and its correlation with spinal deformity in patients with degenerative lumbar scoliosis: a retrospective case-control study. Quant Imaging Med Surg 2024;14(5):3593-3605. doi: 10.21037/qims-23-1668

